

Second Law Thermodynamic Analysis of a Solar Single-Stage Absorption Refrigeration System

J. M. ABDULATEEF, M. A. ALGHOUL, RANJ SIRWAN, A. ZAHARIM & K. SOPIAN

Solar Energy Research Institute (SERI)

University Kebangsaan Malaysia

43600 UKM Bangi, Selangor

MALAYSIA

e-mail: jasimmoh7777@yahoo.com, azami.zaharim@gmail.com, ksopian@eng.ukm.my

Abstract:- This paper deals with thermodynamic simulation and Second-Law analysis of single-stage solar driven absorption refrigeration system operating with Lithium bromide-water solution. A MatLab-based routine was developed to determine thermodynamic properties of the working fluid and the performance simulation results under different operating conditions. The entropy generation of each component and the total entropy generation \dot{S}_{tot} of all the system components as well as the coefficient of performance (COP) of the solar absorption refrigeration system are calculated. The trend in COP and \dot{S}_{tot} with the change in heat exchanger effectiveness, generator, evaporator, absorber and evaporator temperatures are investigated. The results showed that an increase in the generator temperature results in an increase in COP and then decrease while the total entropy generation of the system increased. The COP is more sensitive to changes in the operating conditions of the generator and the evaporator or any other component that affects them, while the total entropy generation considers the effect of all the system components.

Keywords:- Refrigeration; Second law; LiBr-H₂O; Solar energy

1 Introduction

The continuous increase in the cost and demand for energy has led to an extensive research and development for utilizing available energy resources efficiently by minimizing waste energy. Solar cooling technology for air-conditioning and refrigeration applications has received increasing interests as an environmentally-friendly and sustainable alternative. Most of research and development studies regarding solar absorption refrigeration systems (ARSs) deals with the single-stage system type.

It is important to note that system performance can be enhanced by reducing the irreversible losses in the system by using the principles of the second law of thermodynamics. A better understanding of the second law of thermodynamics [1] has revealed that entropy generation minimization is an important technique in achieving optimal system configurations and/or better operating conditions. Some researchers [2,3,4] have used the principles of entropy generation minimization to analyze different systems and to improve the systems performance.

Theoretical and experimental studies on the performance and thermodynamic analysis of ARSs are available in the literature. Chen and Schouten [5] conducted an optimal performance study of an irreversible ARS. They considered irreversibility via

an irreversibility factor and optimized the expression for COP with respect to a number of system parameters. Chua et al. [6] modeled an irreversible ammonia–water absorption chiller by considering the internal entropy production and thermal conductance of the heat exchangers. The model was applied to a single-stage chiller, and the results showed that the highest heat dissipation occurred in the rectifier. Kececiler et al. [7] performed an experimental study on the thermodynamic analysis of a reversible lithium bromide–water ARS.

However, recent analyses of ARSs have included the second law of thermodynamics to provide better understanding of the thermal performance characteristics of each system components. This facilitated the detection of a component with high energy dissipation or irreversible losses. Attention can then be focused on such a component to minimize its irreversible losses. Lee and Sherif [8] applied both the first and the second law of thermodynamics to analyze multi-stage lithium bromide–water ARSs. The second law efficiency of the chillers was calculated from the thermal properties, as well as the entropy generation and exergy of the working fluids. Furthermore, Lee and Sherif [8] used the second law efficiency to quantify the irreversible losses compared to the total entropy

generation, which represents the energy dissipation of the system. Adewusi and Zubair [4] used the second law of thermodynamics to study the performance of single-stage and two-stage ammonia-water ARSs. The entropy generation of each component and the total entropy generation of all the system components as well as the coefficient of performance (*COP*) of the ARSs were calculated. The results show that the two stage system has a higher total entropy generation and *COP*, while the single-stage system has a lower total entropy generation and *COP*.

Apart from the other studies, in this paper a thermodynamic analysis, including First and Second Law analyses, to LiBr-H₂O single-stage ARS powered by solar energy has been carried out. The entropy generation of each component, the total entropy generation of all the components and the *COP* of the ARS are calculated from the thermodynamic properties of the working fluid at different operating conditions using MatLab. The results of total entropy generation of all the components and the *COP* are presented. entropy generation of all the components and the *COP* are then analyzed.

2 System Description

As shown in Fig. 1 the main components of a single effect ARS are the solar collector, generator (*gen*), absorber (*abs*), condenser (*cond*), evaporator (*evp*), pump (*p*), expansion valves (*V1* and *V2*) and a solution heat exchanger (*SHX*). \dot{Q}_{gen} is the heat input rate from the heat source by solar energy to the generator, \dot{Q}_{cond} and \dot{Q}_{abs} are the heat rejection rates from condenser and absorber to the heat sinks, respectively, and \dot{Q}_{evp} is the heat input rate from the cooling load to the evaporator. As shown in Fig. 1, the refrigerant vapor coming from the evaporator (10) is absorbed by liquid solution (6). This liquid solution is then pumped through the solution heat exchanger (*SHX*) (1-2-3). The refrigerant is boiled out of the solution by the addition of heat. Subsequently, the refrigerant goes to the condenser (7-8) and to the evaporator through the expansion valve (*V2*). Finally, the strong lithium liquid solution returns back to the absorber through the solution heat exchanger (*SHX*) and the solution reducing valve (*V1*), respectively (4-5-6).

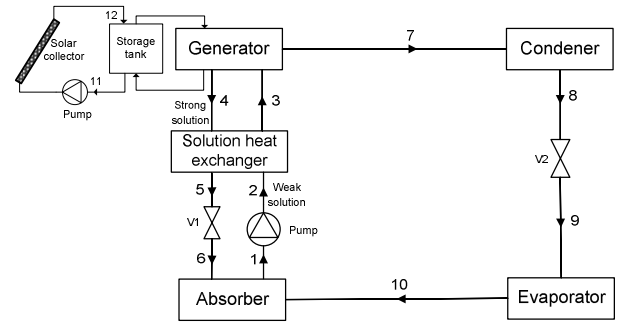


Fig. 1 Schematic of a Solar LiBr-H₂O absorption refrigeration system

3 Thermodynamic Analysis of the System

The governing equations used to evaluating the irreversibility in each component follow.

- Mass balance

$$\sum_e \dot{m}_e = \sum_i \dot{m}_i \quad (1)$$

- Energy balance

$$\dot{Q}_K = \sum \dot{m}_e h_e - \sum \dot{m}_i h_i \quad (2)$$

- Entropy balance

$$\dot{S}_{gen,K} = \sum \dot{m}_e s_e - \sum \dot{m}_i s_i - \frac{\dot{Q}_K}{T_K} \quad (3)$$

where \dot{Q}_K is the heat added to component K at temperature T_K , T_K is the entropic average temperature at which heat flows across the component, K [9,10] and $\dot{S}_{gen,K}$ is the entropy generation of each component K of the ARS.

The performance equations for each of the components considering continuity (mass balance), the first law of thermodynamics (energy balance) and the second law of thermodynamics (entropy generation) are expressed as follows:

Generator

$$\dot{m}_3 = \dot{m}_4 + \dot{m}_7 \quad (4)$$

$$\dot{m}_3 x_3 = \dot{m}_4 x_4 \quad (5)$$

$$\dot{Q}_{gen} = \dot{m}_3 h_3 - \dot{m}_4 h_4 - \dot{m}_7 h_7 \quad (6)$$

$$\dot{S}_{gen} = \dot{m}_3 s_3 - \dot{m}_4 s_4 - \dot{m}_7 s_7 - \frac{\dot{Q}_{gen}}{T_{gen}} \quad (7)$$

Condenser

$$\dot{m}_7 = \dot{m}_8 \quad (8)$$

$$\dot{Q}_{cond} = \dot{m}_7 (h_7 - h_8) \quad (9)$$

$$\dot{S}_{cond} = \dot{m}_7(s_7 - s_8) - \frac{\dot{Q}_{cond}}{T_o} \quad (10)$$

Evaporator

$$\dot{m}_9 = \dot{m}_{10} \quad (11)$$

$$\dot{Q}_{evp} = \dot{m}_9(h_{10} - h_9) \quad (12)$$

$$\dot{S}_{evp} = \dot{m}_9(s_{10} - s_9) - \frac{\dot{Q}_{evp}}{T_{evp}} \quad (13)$$

Absorber

$$\dot{m}_1 = \dot{m}_6 + \dot{m}_{10} \quad (14)$$

$$\dot{Q}_{abs} = \dot{m}_1 h_1 - \dot{m}_6 h_6 - \dot{m}_{10} h_{10} \quad (15)$$

$$\dot{S}_{abs} = \dot{m}_1 s_1 - \dot{m}_6 s_6 - \dot{m}_{10} s_{10} - \frac{\dot{Q}_{abs}}{T_o} \quad (16)$$

Solution pump

$$\dot{m}_1 = \dot{m}_2 \quad (17)$$

$$\dot{W}_p = \dot{m}_1(h_2 - h_1) \text{ or } \dot{W}_p = \frac{\dot{m}_1 v_1 (P_2 - P_1)}{\eta_p} \quad (18)$$

$$\dot{S}_p = \dot{m}_1(s_2 - s_1) \quad (19)$$

Solution heat exchanger (SHX)

$$\varepsilon_{SHX} = \frac{T_4 - T_5}{T_4 - T_2} \quad (20)$$

$$\dot{m}_3 h_3 + \dot{m}_5 h_5 = \dot{m}_2 h_2 + \dot{m}_4 h_4 \quad (21)$$

$$\dot{S}_{SHX} = \dot{m}_3 s_3 + \dot{m}_5 s_5 - \dot{m}_2 s_2 - \dot{m}_4 s_4 \quad (22)$$

Solution expansion valve (V1)

$$\dot{m}_5 = \dot{m}_6 \quad (23)$$

$$\dot{m}_5 h_5 = \dot{m}_6 h_6 \quad (24)$$

$$\dot{S}_{V1} = \dot{m}_5(s_6 - s_5) \quad (25)$$

Refrigerant expansion valve (V2)

$$\dot{m}_8 = \dot{m}_9 \quad (26)$$

$$\dot{m}_8 h_8 = \dot{m}_9 h_9 \quad (27)$$

$$\dot{S}_{V2} = \dot{m}_8(s_9 - s_8) \quad (28)$$

Solar collector

$$\dot{m}_{11} = \dot{m}_{12} \quad (29)$$

$$\dot{Q}_u = \dot{m}_{11}(h_{12} - h_{11}) \quad (30)$$

$$\dot{S}_{sc} = \dot{m}_{11}(s_{12} - s_{11}) - \frac{\dot{Q}_u}{T_{sc}} \quad (31)$$

The system performance is measured by the coefficient of performance (COP):

$$COP = \frac{\dot{Q}_{evp}}{\dot{Q}_{gen} + \dot{W}_p} \quad (32)$$

$$\dot{S}_{tot} = \dot{S}_{gen} + \dot{S}_{cond} + \dot{S}_{evp} + \dot{S}_{abs} + \dot{S}_p + \dot{S}_{SHX} + \dot{S}_{V1} + \dot{S}_{V2} + \dot{S}_{sc} \quad (33)$$

were given to the routine as initial inputs/data including solar collector conditions, component temperatures, pump efficiency and effectiveness of heat exchanger. With the given parameters, the thermodynamic properties of the fluid at all reference points in the cycle were calculated. In this work, the thermodynamic properties of the LiBr-H₂O mixture are taken from the correlations provided by Patek and Klomfar [11]. The property data of the liquid water and vapor were determined by the Talbi and Agnew [12] equations. Solar collector performance calculations were taken based on Abdulateef [13].

Simulations are carried out for pump efficiency =80%, while the effectiveness of the SHX is 70%. Condensation temperature is equal to the absorber temperature. Condensation temperature is varied in the following range: $T_{cond} = 25\text{--}45^\circ\text{C}$. Evaporation temperature is varied in the following range: $T_{evp} = 3\text{--}15^\circ\text{C}$. Generation temperature is varied in the following range: $T_{gen} = 60\text{--}100^\circ\text{C}$. The mass flow rate of solution through the pump is 1 kg/min and the environment temperature, $T_o = 25^\circ\text{C}$ was taken. Table 1 shows the thermodynamic properties of the solar single-stage ARS at all state points for the average of three selected days. The performance results has presented in Table 2.

Table 1 State points for the solar absorption refrigeration system and the calculated results ($T_{gen}=80^\circ\text{C}$, $T_{evp}=5^\circ\text{C}$, $T_{cond}=T_{abs}=35^\circ\text{C}$)

| Point | T(°C) | P(kpa) | h(kJ/kg) | s(kJ/kg.K) | \dot{m} (kg/sec) | x(kg/kg sol) |
|-------|-------|--------|----------|------------|--------------------|--------------|
| 1 | 35 | 0.873 | 85.331 | 0.211 | 0.016 | 0.553 |
| 2 | 35 | 5.629 | 85.331 | 0.221 | 0.016 | 0.553 |
| 3 | 62 | 5.629 | 140.314 | 0.382 | 0.016 | 0.553 |
| 4 | 80 | 5.629 | 195.808 | 0.450 | 0.0146 | 0.603 |
| 5 | 48.5 | 5.629 | 135.625 | 0.272 | 0.0146 | 0.603 |
| 6 | 48.5 | 0.872 | 135.625 | 0.279 | 0.0146 | 0.603 |
| 7 | 80 | 5.629 | 2650.317 | 8.611 | 0.0013 | 0 |
| 8 | 35 | 5.629 | 146.772 | 0.495 | 0.0013 | 0 |
| 9 | 5 | 0.872 | 146.772 | 0.515 | 0.0013 | 0 |
| 10 | 5 | 0.872 | 2510.452 | 9.025 | 0.0013 | 0 |

Table 2 Performance results of for the solar absorption refrigeration system and the calculated results

($T_{gen}=70\text{--}90^\circ\text{C}$, $T_{evp}=5^\circ\text{C}$, $T_{cond}=T_{abs}=35^\circ\text{C}$)

| T(°C) | \dot{Q}_{evp} (kW) | \dot{Q}_{cond} (kW) | \dot{Q}_{abs} (kW) | \dot{Q}_{gen} (kW) | \dot{W}_p (kW) | \dot{S}_{tot} (kW/K) | COP |
|-------|----------------------|-----------------------|----------------------|----------------------|------------------|------------------------|-------|
| 70 | 0.225 | 0.236 | 0.586 | 0.602 | 0.00059 | 0.00388 | 0.374 |
| 80 | 3.142 | 3.328 | 3.962 | 4.151 | 0.00059 | 0.02581 | 0.756 |
| 90 | 5.547 | 5.919 | 6.863 | 7.238 | 0.00059 | 0.0447 | 0.766 |

Fig. 2 shows the effect of the generator temperature on COP and total entropy generation of the ARS. This figure shows that an increase in the generator temperature results in an increase in COP

and then decreases while the total entropy generation of the system increases. There is an optimal value of generator temperature which gives maximum COP . It is important to emphasize, that the COP is sensitive to the output and input energies alone.

Fig. 3 shows the effect of the evaporator temperature on COP and total entropy generation of the ARS. This figure shows that an increase in the evaporator temperature results in an increase in both COP and total entropy generation of the system. The COP is more sensitive to changes in the operating conditions of the generator and the evaporator or any other component that affects them, while the total entropy generation considers the effect of all the system components.

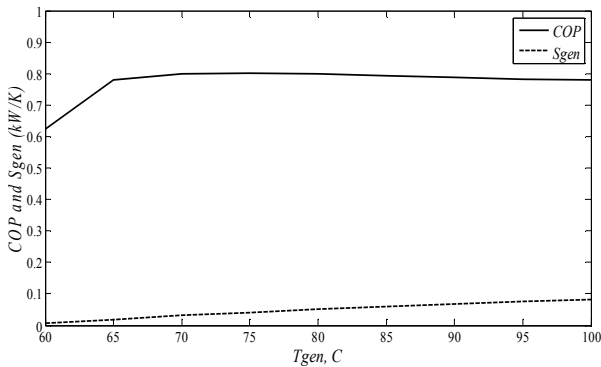


Fig. 2 Effect of T_{gen} on COP and \dot{S}_{tot}

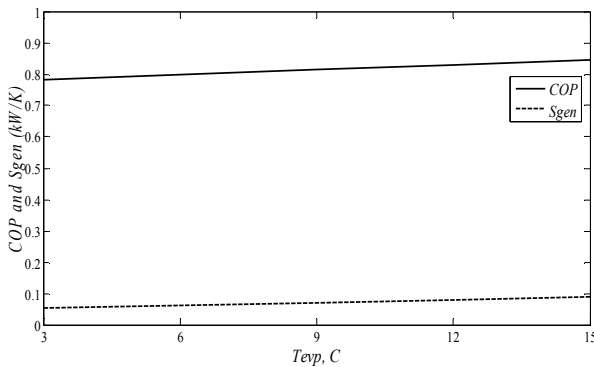


Fig. 3 Effect of T_{evp} on COP and \dot{S}_{tot}

Fig. 4 shows the effect of absorber outlet temperature on COP and total entropy generation of the ARS. Fig. 5 presents the effect of condenser outlet temperature on COP and total entropy generation of the ARS. Both figures show that an increase in temperature results in a decrease in both COP and the total entropy generation of the systems.

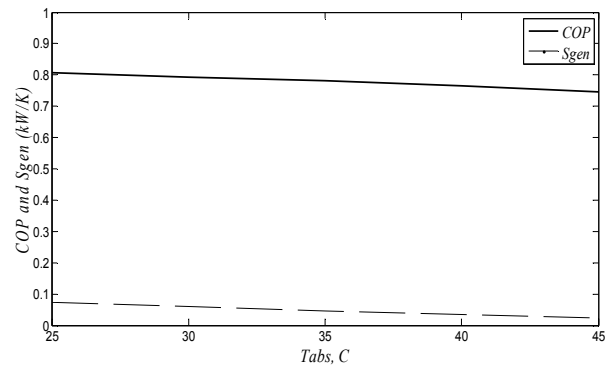


Fig. 4 Effect of T_{abs} on COP and \dot{S}_{tot}

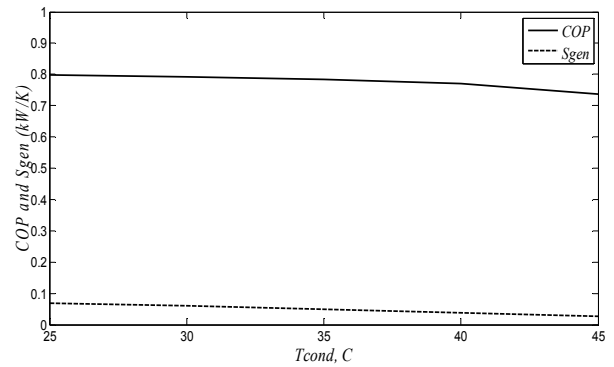


Fig. 5 Effect of T_{cond} on COP and \dot{S}_{tot}

Fig. 6 presents the effect of the solution heat exchanger effectiveness on COP and \dot{S}_{tot} . As expected, the COP of solar single-stage ARS increased with an increase in the effectiveness, but the effect of changes in the effectivenesses is negligible on the total entropy generation.

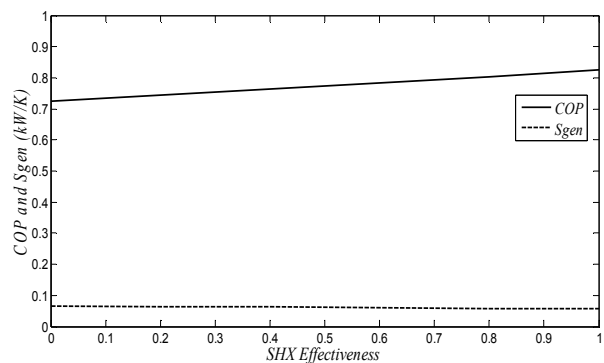


Fig. 6 Effect of \square_{SHX} on COP and \dot{S}_{tot}

5 Conclusions

Second law analysis provides an alternative view of system performance and provides an insight that the first law method cannot. It is proved to be a simple and effective tool, by providing information about how losses at different components are

interdependent and where a given design should be modified for best performance. In this work, the second law of thermodynamics is used to study the performance of solar single-stage ARSs when some parameters are varied.

The entropy generation of each component, the total entropy generation \dot{S}_{tot} of all components and the COP of the solar ARS are calculated from the thermodynamic properties of the working fluid at different operating conditions using MatLab. The results showed that an increase in the generator temperature involves in an increase in COP and then decreases while the total entropy generation of the system increases. There is an optimal value of generator temperature which gives maximum COP . In case of absorber and condenser, the results showed that an increase in temperature results in a decrease in both COP and the total entropy generation of the systems. The COP is more sensitive to changes in the operating conditions of the generator and the evaporator or any other component that affects them, while the total entropy generation considers the effect of all the system components.

Acknowledgment

The authors would like to thank the Solar Energy Research Institute (SERI), University Kebangsaan Malaysia, for support.

Nomenclature

| | |
|-----------------|--------------------------------------|
| COP | coefficient of performance |
| h | enthalpy (kJ/kg) |
| \dot{m} | mass flow rate (kg/s) |
| P | pressure (kPa) |
| \dot{Q} | thermal energy rate (kW) |
| s | entropy (kJ/kg .K) |
| SHX | solution heat exchanger |
| \dot{S} | entropy generation rate (kW/K) |
| \dot{S}_{tot} | total entropy generation rate (kW/K) |
| T | temperature (°C) |
| v | specific volume (m ³ /kg) |
| \dot{W} | pump power (kW) |
| x | Lithium bromide mass fraction |
| ε | heat exchanger effectiveness |

Subscripts

| | |
|--------|------------|
| abs | absorber |
| $cond$ | condenser |
| evp | evaporator |

| | |
|-------|--|
| gen | generator |
| i | state point or index $i=1, 2, 3 \dots$ |
| o | ambient condition |
| p | pump |
| sc | solar collector |
| u | useful |
| SHX | solution heat exchanger |
| tot | total |
| V | expansion valve |

References:

- [1] Lieb EH, Yngvason J. A fresh look at entropy and the second law of thermodynamics. Phys Today2000;53(4):32–6.
- [2] Ogulata RT, Doba F. Experiments and entropy generation minimization of a cross-flow heat exchanger. Int.J.Mass.Transfer 1998;41(2):373–81.
- [3] Vargas J, Bejan A, Siems D. Integrative thermodynamic optimization of cross-flow heat exchanger for an aircraft environmental control system. J Heat transfer 2001;128:760–9.
- [4] Adewusi S.A., Syed M. Zubair. Second law based thermodynamic analysis of ammonia–water absorption systems. Energy Conversion and Management 2004 ;45:2355–2369.
- [5] Chen J, Schouten JA. Optimum performance characteristics of an irreversible absorption refrigeration system. . Energy Conversion and Management 1998;39:999–1007.
- [6] Chua HT, Toh HK, Ng KC. Thermodynamic modeling of an ammonia/water absorption chiller. Int J Refrig 2002;25:896–906.
- [7] Kececiler A, Acar HI, Dogan A. Thermodynamic analysis of absorption refrigeration system with geothermal energy: an experimental study. Energy Conversion and Management 2000;41:37–48.
- [8] Lee SF, Sherif SA. Second-law analysis of multi-effect lithium bromide/water absorption chillers. ASHRAE Trans 1999;105(1):1256–66.
- [9] Schaefer L.A., Delano A. and Shelton S.V.. Second Law Study of the Einstein Refrigeration Cycle. GWW School of Mechanical Engineering, Georgia Institute of Technology, 1999.
- [10] Herold K.E, Radermaeher R, Klein , S.A. Absorption Chillers and Heat Pumps. CRC Press, Boca Raton, 1996.
- [11] Patek J, Klomfar J. A computationally effective formulation of the thermodynamic properties of LiBr–H₂O solutions from 273 to 500 K over

- full composition range. *International Journal of Refrigeration* 2006;29:566–578.
- [12] Talbi MM, Agnew B. Exergy analysis: an absorption refrigerator using lithium bromide and water as the working fluids. *Applied Thermal Engineering* 2000;20:619-630.
- [13] Abdulateef, J.M. 2010. Combined solar-assisted ejector absorption refrigeration system. Ph. D. thesis. Solar Energy Research Institute (SERI). Universiti Kebangsaan Malaysia.